Additive Manufacturing 17 (2017) 169–175

Contents lists available at ScienceDirect

Additive Manufacturing

journal homepage: www.elsevier.com/locate/addma

Full Length Article

Electron beam melted scaffolds for orthopedic applications

Ibrahim Eldesouky [a,*], Ola Harrysson [b], Harvey West [b], Hassan Elhofy [a]

[a] Department of Industrial Engineering and Systems Management, Egypt-Japan University of Science and Technology, New Borg El Arab, 21934, Egypt
[b] Center for Additive Manufacturing and Logistics, Edward P. Fitts Department of Industrial & Systems Engineering, North Carolina State University, Raleigh, NC 27695, USA

ARTICLE INFO

Article history:
Received 20 September 2016
Received in revised form 8 July 2017
Accepted 22 August 2017
Available online 26 August 2017

Keywords:
Electron beam melting
Porous structure
Reentrant
Ti6Al4V

ABSTRACT

Ti6Al4V porous scaffolds of two unit cell geometries (reentrant and cubic) were investigated as candidates for load-bearing biomedical applications. Samples were fabricated using an Arcam A2 electron beam melting (EBM) machine and evaluated for geometric deviation from the original CAD design using a digital optical microscope. The mass and bounding volume of each sample were also measured to calculate the resulting relative density. The scaffolds were loaded in compression in the build direction to determine the relative modulus of elasticity and ultimate compressive load. Experimental results were used to calculate the Gibson and Ashby relation parameters for the studied unit cell geometries. The results suggest that samples with the cubic unit cell geometries, with struts oriented at an angle of 45° to the loading direction, exhibited higher stiffness than samples with the reentrant unit cell geometry at equivalent relative densities. A cubic scaffold is verified to withstand high compressive loads (more than 71 kN) while having an approximate pore size in the range of 0.6 mm. These characteristics demonstrate its suitability for load bearing biomedical implants.

1. Introduction

The use of porous metal structures has expanded to a wide variety of component designs in aerospace [1], automotive [2], biomedical [3,4], and even fashion [5]. The motivation behind this research is based on the biomedical applications of porous metal structures.

Currently, load-bearing implants are manufactured using materials such as stainless steel, cobalt-chromium, tantalum, or titanium alloys. The significant mismatch in stiffness between the solid metal implants and bone can lead to stress shielding, bone resorption, and implant failure [6]. Aseptic loosening due to stress shielding remains one of the leading causes of joint replacement failure [7]. The stiffness of porous metal structures can be tailored by controlling the relative density of the bulk material, and this approach has been demonstrated to reduce stress shielding [8].

Manipulation of mesoscale unit cell geometry can give rise to unique macro-scale properties. For instance, unit cell lattice structures exhibiting negative Poisson's ratios were first introduced in the 1980s [9]. These are characterized by their lateral expansion during uniaxial tension and lateral contraction during uniaxial compression. Several mathematical models have been developed for estimating the mechanical characteristics of reentrant structures [10,11]. However, early applications for metallic auxetic structures were not thoroughly studied owing, in part, to the difficulty associated with their manufacturing. With the development of metal additive manufacturing techniques, several geometrical combinations of reentrant unit cell scaffolds were fabricated and tested using EBM [12]. Accordingly, a reentrant structure can be tuned to have a stiffness similar to that of the human bone, with the right combination of geometrical parameters (reentrance angle and H/L ratio). The more the reentrance angle approaches 90°, the more the stiffness decreases. In this regard, a reentrance angle of 70° was selected for initial testing to obtain stiffness values near the range of natural human bone.

Other cellular geometries including cubic scaffolds were studied in previous research work using 316 stainless steel, cobalt chromium, Titanium alloys, and other polymeric materials [13–19]. Electron beam melted Ti6Al4 V cubic structures with compressive strength, and elastic modulus comparable to those of trabecular and cortical bone were tested in the literature [13,17]. However, all the tested scaffolds had a pore size equal to or larger than 1 mm which is not recommended for bone ingrowth applications [20]. The cubic structures also have higher specific strength than other reported metallic stochastic foams of identical specific stiffness

* Corresponding author at: Department of Industrial Engineering and Systems Management, Egypt-Japan University of Science and Technology, New Borg El Arab, 21934, Egypt.
E-mail address: ibrahim.desouky@ejust.edu.eg (I. Eldesouky).

http://dx.doi.org/10.1016/j.addma.2017.08.005
2214-8604/

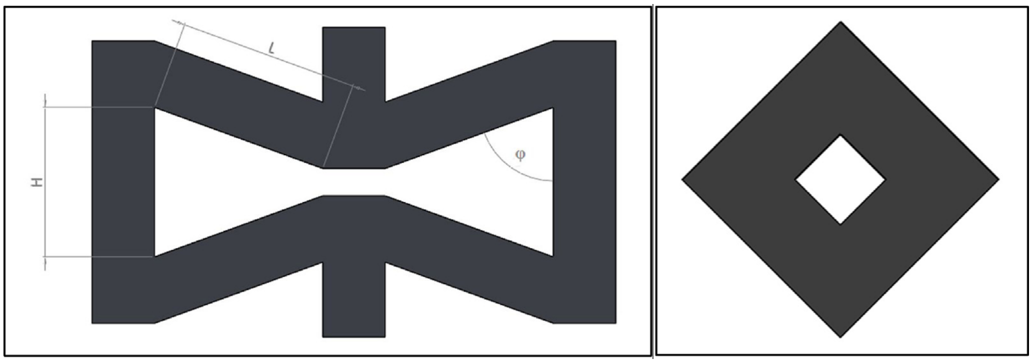

Fig. 1. The reentrant (left) and cubic (right) cell configurations.

[21]. Four Cobalt Chromium porous structures of different cubic topologies were tested under compression, the cellular structures with inclined bearing struts and horizontal arms have the minimum stress concentration among the four cell topologies [19]. Cubic Ti6Al4 V structures were also studied as candidates for cage spacers used in spine surgery [22].

Another research trend is testing the Effect of pore size and shape on bone ingrowth into porous titanium implants. In this regard, high cell penetration depth was obtained in a cubic structure with a pore size of 700 μm [23].

Mathematical models for predicting the mechanical behavior of porous scaffolds were found to be in good agreement with experimental results for small relative density values (less than 0.05). However, for large relative density values (more than 0.15), the results from the mathematical models deviated significantly from actual experiments [24]. The deviation is related to the several simplifying assumptions that are often incorporated in the mathematical models [25].

While Finite Element (FE) models are considered more accurate than mathematical models in predicting the mechanical properties of porous scaffolds, FE modeling requires a specific FE model for each defined porous structure which requires specific computation tools [25]. Also, modeling of large lattice structures is not possible as the number of elements becomes very large. Additionally, the geometrical deviation that is caused by manufacturing techniques significantly influenced the mechanical properties of the porous scaffolds and should, therefore, be implemented in FE models using, for example, a micro computed tomography scan of the actual test sample [26].

Although metal additive manufacturing techniques are supposed to provide the capability of producing structures with any possible design, not all virtual designs can be translated into actual products [27]. Some of the limitations of the process include the need for support structures for the overhanging struts in the scaffolds when the unit cells have a large size and powder adhesion on the struts. Another problem that still faces scaffolds produced by the electron beam melting is the removal of excess powder that is sintered within the pores of the scaffold [28].

This study aims at designing, producing and testing porous structures with different porosities. Effective structures should build completely without using supports, provide clearance for removing excess powder, and have a minimum deviation from the original design. The tested structures can be incorporated into the design of new functionally graded porous orthopaedic implants. The mechanical performance of cubic and reentrant scaffolds were evaluated under compression to determine the superior scaffold geometry regarding the obtained relative modulus of elasticity compared to relative density.

2. Methods

Ten design configurations (five reentrant, and five cubic) were designed using a CAD software package (SolidWorks 2015, Dassault Systems, Waltham, MA, USA). The reentrant structure is characterized by the reentrance angle (φ) and the ratio of the vertical strut length (H) to the reentrant strut length (L) as demonstrated in Fig. 1. Each unit cell design was replicated to fill a cube with an edge length of approximately 25 mm. A square strut cross section was chosen to improve the computational efficiency [20]. Tables 1 and 2 present the design values for the different geometrical combinations of cubic (C1-C5) and reentrant (A1-A5) unit cells respectively.

Three replications of each design combination were produced in a single EBM run. Samples were arranged on a 190 mm square build platform, spaced at a minimum distance of 4 mm apart, using an STL processing software (Magics 19, Materialise, Leuven, Belgium). Samples with cubic unit cell geometries were oriented at 45° to the vertical plane to ensure self-supporting geometries during the AM process. Tilting the sample relative to the build platform was avoided since it negatively affects the mechanical properties of the obtained scaffold [29]. STL files were exported to the Arcam Build Assembler™ software (Arcam, Mölndal, Sweden) for slicing at 50 μm intervals.

The samples were fabricated using an Arcam A2 EBM machine. The material utilized was gas atomized Ti6Al4 V powder with a nominal size distribution ranging from 45 to 105 μm [30]. The standard parameter set for Ti6Al4 V lattice structures with 50 μm layers was used (Arcam Build Control Software V3.2, SP2, Ti6Al4 V "network," Arcam, Mölndal, Sweden). Sintered powder was removed from the samples using the Arcam powder recovery system, which is an abrasive blasting process that uses the Ti6Al4 V powder as

Table 1
Design values for different geometrical design configurations of cubic unit cells.

Cubic structure	Nominal Strut Thickness (mm)	Pore Size (mm)	Nominal relative density (g/cm^3)	Design bounding volume (Height × Length × Depth) (mm)
C1	0.20	1.50	0.04	24.29 × 24.29 × 24
C2	0.25	1.25	0.08	25.79 × 25.79 × 24.25
C3	0.50	1.50	0.16	23.35 × 23.35 × 24.5
C4	1.00	0.80	0.56	24.36 × 24.36 × 24.4
C5	3.00	3.80	0.37	23.48 × 23.48 × 23.4